Asian Journal of Chemistry; Vol. 34, No. 1 (2022), 216-222

ASIAN JOURNAL OF CHEMISTRY

https://doi.org/10.14233/ajchem.2022.23498

Green Synthesis, Characterization, Antioxidant, Antibacterial and Dye Degradation of Silver Nanoparticles using *Combretum indicum* Leaf Extract

ARNANNIT KUYYOGSUY[1,*], PAWEENA PORRAWATKUL[1], RUNGNAPA PIMSEN[1], PRAWIT NUENGMATCHA[1], BENJAWAN NINWONG[1], NICHAPA RATTANAKOMON[1] and SAKSIT CHANTHAI[2]

[1]Nanomaterials Chemistry Research Unit, Department of Chemistry, Faculty of Science and Technology, Nakhon Si Thammarat Rajabhat University, Nakhon Si Thammarat 80280, Thailand
[2]Materials Chemistry Research Center, Department of Chemistry and Center of Excellence for Innovation in Chemistry, Faculty of Science, Khon Kaen University, Khon Kaen 40002, Thailand

*Corresponding author: Tel/Fax: +6675-377-443; E-mail: arnannit.k@gmail.com

Received: 25 August 2021; *Accepted*: 10 October 2021; *Published online*: 16 December 2021; AJC-20638

Silver nanoparticles were synthesized by bioreduction of silver nitrate using the aqueous leaf extract of *Combretum indicum* (*CI*-AgNPs). The synthesized *CI*-AgNPs exhibited a distinct absorption peak at 414 nm in UV-vis spectroscopy. Various parameters such as pH, temperature and time were optimized using spectrophotometry. The particle size of the *CI*-AgNPs was 48 nm as evaluated from the laser particle size analyzer. The XRD and EDX analyses confirmed the presence of silver in silver nanoparticles. Synthesized *CI*-AgNPs revealed significant antioxidant, antimicrobial (against *Escherichia coli* and *Staphylococcus aureus*) and photocatalytic (against methylene blue under sunlight irradiation) activities. Thus, an eco-friendly method was developed to synthesize silver nanoparticles using the *C. indicum* leaf extract.

Keywords: Silver nanoparticles, *Combretum indicum*, Green synthesis, Antioxidant, Antibacterial, Photocatalytic activity.

INTRODUCTION

Nanotechnology has been an important branch of modern investigations to synthesize, design and manage particle structures ranging from about 1-100 nanometers [1]. Nanoparticles are interesting materials because of their excellent properties, which allow their use in a broad range of applications in many fields such as biotechnology, sensors, catalyst, chemical industries, food, electronics, cosmetics, pharmaceuticals, materials science, environmental health and energy science [2]. The literature cites numerous ways to synthesize nanoparticles [3-6]. However, some disadvantages of these methodologies include high costs, toxic substances, high pressure and temperature. For this reason, the green synthesis methodology was developed as an alternative to the chemical synthesis procedure [7-9]. The methodology of green synthesis is fundamental because it has the advantages of being eco-friendly, low-cost and easy to produce.

Metal nanoparticle synthesis by the green methodology is performed in one step at ambient temperature [10,11]. Therefore, it is relatively easy and eco-friendly. Among the numerous metal nanoparticles, silver nanoparticles (AgNPs) play a major role in biology and medical science. AgNPs have a high level of antibacterial activity and are listed as antimicrobial agents. Numerous studies of AgNPs synthesized through green synthesis methods report their anticancer, antifungal, antimicrobial properties and antioxidant activity against free radicals such as DPPH [12,13]. Moreover, AgNPs can be applied to degrade organic pollutants such as dyes [14,15]. AgNPs have been synthesized by numerous methods such as microwave processes, electrical chemistry, hydrothermal and green chemistry [16-18]. However, the green synthesis of AgNPs employed algae, bacteria and plants [14,19,20]. Particularly, the plant extracts used to synthesize AgNPs included *Camellia sinensis*, *Crataegus pentagyna, Punica granatum* and *Pistacia atlantica* [8,12,21].

Lep Mue Naang (*Combretum indicum* L. DeFilipps) belongs to the genus *Combretum*, which originated in Southeast Asia and tropical Africa. It is mostly a sub-woody climber or a scram-

bling shrub with red flower clusters. *C. indicum* has been used as a medical plant wherein the decoction of the fruit, seed or root can be used as an anthelmintic to treat infections with parasitic worms or help alleviate the symptoms of diarrhea. In Thailand, the seeds are used as anthelmintics, while the leaf is used to heal abscesses [22]. Moreover, it is reported to exhibit antimicrobial activity [23], anti-inflammatory activity [24], antidiabetic activity [25], antipyretic activity [26], antihyperlipidemic activity [27], antitumor activity [28]. It also contains phenolic compounds that exhibit antioxidant activity [22]. These biomolecules are found in the structure of the plant extract and play a major role in reducing, capping and stabilizing metal salts. Many studies reported that biomolecules, particularly flavonoids, play an important role in metal salt reduction [29].

The current study aimed to provide a green synthesis of AgNPs as an alternative method to the conventional pathway. AgNPs were synthesized using the *C. indicum* leaf extract. The synthesized AgNPs were analyzed by SEM, XRD, TEM, laser particle size analyzer (LPSA), FTIR and UV-vis techniques. Finally, the antioxidant and antibacterial activities and dye degradation properties of the synthesized AgNPs were evaluated.

EXPERIMENTAL

The leaves of *Combretum indicum* were obtained from Thung Prang, Sichon District, Nakhon Si Thammarat Province, Thailand. All chemicals were of the analytical grade and purchased from Sigma-Aldrich. Microbial strains were obtained from Nakhon Si Thammarat Rajabhat University. All materials were sterilized at 121 ºC and 15 psi pressure for 30 min before determining antibacterial activity.

Extraction of *C. indicum* (*CI*) leaf extract: For extraction, 10.0 g of dried *C. indicum* leaf was weighed, cut into small pieces and mixed with 150 mL of distilled water at 60 ºC for 2 h. The extract was filtered and used for the synthesis of nanoparticles.

Phytochemical analysis of *C. indicum* leaf extract: The qualitative phytochemical analysis of the aqueous leaf extracts of *C. indicum* was carried out with reference to anthraquinones, flavonoids, steroids, terpenoids, saponins, alkaloids and tannins by following the standard methods [30,31].

Green synthesis of AgNPs from *C. indicum* leaf extracts (*CI*-AgNPs): Briefly, 2 mL of *C. indicum* leaf extract was mixed with 18 mL of a 1 mM $AgNO_3$ solution at 60 ºC under vigorous stirring for 3 h. Next, the obtained solution was heated in an oil bath with continuous stirring. The colour change from light yellow to brown indicated the successful synthesis of AgNPs. Further, the synthesized particles were rinsed several times with distilled water and left to dry in a hot air oven for 24 h. A procedure for the optimization of parameters was standardized. It included three factors: pH (pH of extract: 5, 7 and 9), time of extraction (1, 2, 3 and 5 h) and temperature for extraction (room temp., 40 and 60 ºC). The optimized parameters resulted in achieving the best size and morphology of the synthesized AgNPs.

Characterization of biosynthetic silver nanoparticles (*CI*-AgNPs): The synthesis of AgNPs was confirmed by recording the absorbance spectra of synthesized *CI*-AgNPs in the wavelength range of 250-750 nm using a UV-vis spectrophotometer. The morphology and particle size of the synthesized *CI*-AgNPs were analyzed using SEM (scanning electron microscopy), EDX (energy-dispersive X-ray spectroscopy), TEM (transmission electron microscope) and LPSA (laser particle size analyzer). The XRD platform was investigated using an XRD diffractometer equipped with an X-ray generator containing Cu$K\alpha$ radiation and operated at 40 mA. The functional groups of the *C. indicum* leaf extract were related to the reduced $AgNO_3$ metal salts and stabilized the AgNPs. They were characterized by FTIR (Perkin-Elmer) in the 4000 to 500 cm^{-1} region.

Determination of antioxidant effect of *CI*-AgNPs by DPPH: To evaluate the antioxidant activity of biosynthetic *CI*-AgNPs, 2 mL of 2×10^{-4} mM 2,2-diphenyl-1-picrylhydrazyl (DPPH) in 95% ethanol was added to 1 mL of various concentrations of *C. indicum* aqueous leaf extracts. The samples were incubated in the dark for 5 min and their absorbance was determined at 518 nm. Here, 95% ethanol was served as the blank, while ascorbic acid served as the antioxidant standard. The antioxidant capability against the DPPH radical was calculated using the following formula (1):

$$\text{DPPH scavenged (\%)} = \frac{A_c - A_s}{A_c} \times 100 \quad (1)$$

where A_c and A_s indicate the absorbance values for the control and test sample, respectively (after 30 min and at 518 nm). The data were analyzed and the IC_{50} values were measured using the linear regression equation [32].

Antibacterial assay of *CI*-AgNPs: The antibacterial activity of the synthesized *CI*-AgNPs was evaluated using the agar well diffusion technique. The experimental pathogens included *Escherichia coli* and *Staphylococcus aureus*. The prepared microbial suspensions with 0.5 McFarland turbidity standards were spread onto Mueller Hinton Agar (MHA) under completely sterile conditions using a sterile cotton swab. Then, 80 µL of AgNPs were added to the wells and subsequently incubated at 37 ºC for 24 h. Distilled water was served as the negative control, while chloramphenicol (30 µg/mL) was a positive control. The zone of growth inhibition was determined from the diameter of the bacterial growth around the wells.

Catalyst activity: The catalytic activity of synthesized silver nanoparticles was evaluated by the method of methylene blue reduction. Briefly, 30 mg of Ag nanocatalyst was dispersed into 15 mL of 0.06 mM methylene blue dye. AgNPs, a photocatalyst and the methylene blue dye reached adsorption equilibrium under magnetic stirring for 40 min. Further, the absorbance by the methylene blue solution was evaluated at 664 nm using UV-vis spectroscopy. The solution without the AgNPs was used as the control set.

RESULTS AND DISCUSSION

Phytochemical analysis of *C. indicum* leaf extract: The results of the phytochemical analysis of *C. indicum* leaf extract are presented in Table-1. Several secondary metabolites such as flavonoids, steroids, terpenoids, saponins, alkaloids and tannins were identified in the leaf extract; no anthraquinones

TABLE-1
PHYTOCHEMICAL ANALYSIS OF THE LEAF EXTRACT OF *C. indicum*

Phytochemical compounds	Leaf extract
Anthraquinones	Absent
Flavonoids	Present
Steroids	Present
Terpenoids	Present
Saponins	Present
Alkaloids	Present
Tannins	Present

were detected. Other studies have reported the presence of alkaloids, some amount of glycosides, tannins, flavonoids and terpenoids from the leaves of *C. indicum* [26]. The Iraqi plant (*Quisqualis indica* L.) composes tannins, saponins, flavonoids, coumarin and terpene, while alkaloids and steroids are observed as minor components [33]. The crude extracts of the African peach (*Nauclea latifolia*) revealed the presence of saponins, flavonoids, alkaloids, terpenoids, anthraquinones, steroids, glycosides and tannins [34]. These biomolecules, particularly the flavonoids and phenolic compounds, exhibit an active role as reducing agents, while the proteins and some other phytochemicals act as capping and reducing agents during the green synthesis of AgNPs. The electrons released from the phenolic compounds and flavonoids break the O-H bond and reduce the Ag^+ ions to Ag^0 [35].

Optimization of synthesis of *CI*-AgNPs: The absorption spectrum of the synthesized *CI*-AgNPs was analyzed in the range of 250-750 nm using a UV-vis spectrophotometer. The position of the surface plasmon resonance (SPR) band depends on the morphology and size. According to Mie's theory, a single SPR band results in a spherical shape of the nanoparticle, while two or more plasmon bands present various shapes of nanoparticles. The SPR plasmon peaks of the AgNPs depended on various factors such as the particle size and shape [36]. Thus, reaction conditions like the pH, time and temperature of incubation were optimized to check their influence on the conformation, size and distribution of the AgNPs. In the current study, no shift was observed during the green synthesis indicated the stability of the synthesized AgNPs (Fig. 1).

The pH values affect the morphology and size of the nanoparticles. The *CI*-AgNPs were prepared from *C. indicum* leaf extract at various pH values (pH: 3, 5, 7 and 9) (Fig. 1a). The UV-visible spectra demonstrated that the plasmon absorption band increased with an increase in pH. The band also shifted to 414 nm when the pH changed from 5 to 9 because of increased *CI*-AgNP preparation and reduced reaction rate. Thus, the maximum absorbance of *CI*-AgNPs was recorded at pH-9, which considered as the optimum pH for all the further experiments.

The progress of AgNPs reduction was evaluated at different times (1, 2, 3 and 5 h) and recorded by the UV-visible spectra (Fig. 1b). The reduction increased with increasing contact times (1 to 3 h). However, the reduction was similar at 3 h and 5 h. Therefore, the optimum reaction time was considered as 3 h as it displayed the maximum absorbance and complete bio-reduction of $AgNO_3$ was observed. The UV-visible absorption spectra demonstrated that the AgNPs prepared by this process were stable and did not aggregate in the optimum time.

Temperature is an important parameter that controls the particle size and the morphology of nanoparticles. Therefore, the green synthesis of *CI*-AgNPs was attempted at different temperatures (room temperature, 40 ºC and 60ºC). The optimum temperature for the preparation of *CI*-AgNPs was identified using UV-vis spectroscopy in the range of 250-750 nm (Fig. 1c). The plasmon resonance peak of *CI*-AgNPs shifted to a higher wavelength upon an increase in the particle diameter (Fig. 1c). Thus, the optimized temperature for the synthesis of *CI*-AgNPs was found to be 60 ºC. These optimum conditions (pH, time and temperature) were used for further studies.

XRD of *CI*-AgNPs: The XRD pattern of the AgNPs was obtained by green synthesis using the *C. indicum* leaf extract (*CI*-AgNPs) and optimum parameters (pH-9, temperature of 60 ºC and time of incubation 3 h) is shown in Fig. 2. The results showed that the diffraction peaks corresponded to the Bragg's equation (1 1 1), (2 0 0), (2 2 0) and (3 1 1) and planes that were relevant to $2\theta = 38º, 43º, 64º$ and 77º, respectively. Meanwhile, the XRD pattern data of the *CI*-AgNPs was submitted to the XRD database of the Joint Committee on Powder Diffraction Standards (JCPDS) with file number 87-0717.

SEM-EDX studies: The scanning electron microscopy (SEM) image used to estimate the shape and particle size of the nanomaterials (Fig. 3) indicated the presence of several spherical shapes that were mostly aggregated. The energy-dispersive X-ray (EDX) technique of *CI*-AgNPs analyzed the elemental composition and the presence of Ag, O, C and Mg was confirmed. A higher percentage of the Ag element was visible in the EDX analysis of the *CI*-AgNPs (Fig. 4).

TEM studies: The AgNPs showed a spherical shape and uniform distribution under a transmission electron microscope

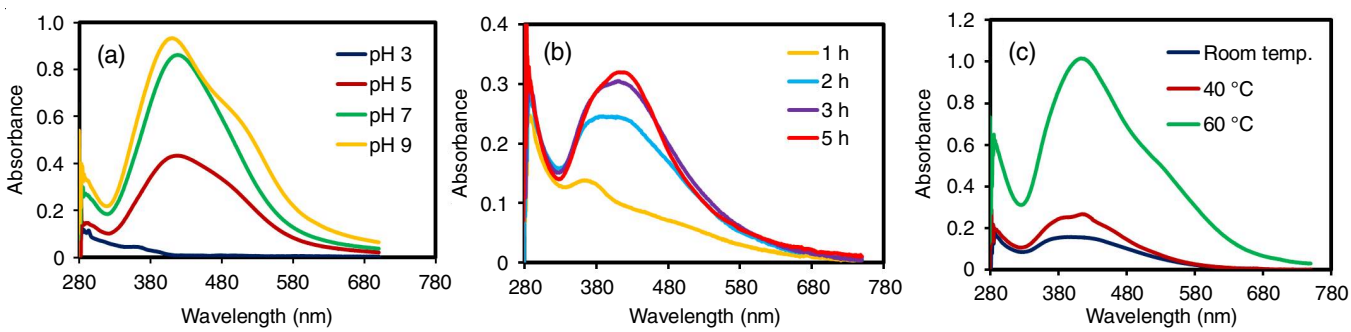

Fig. 1. UV-vis spectra of the synthesized *CI*-AgNPs for optimization at different pH (a), time (b) and temperature (c)

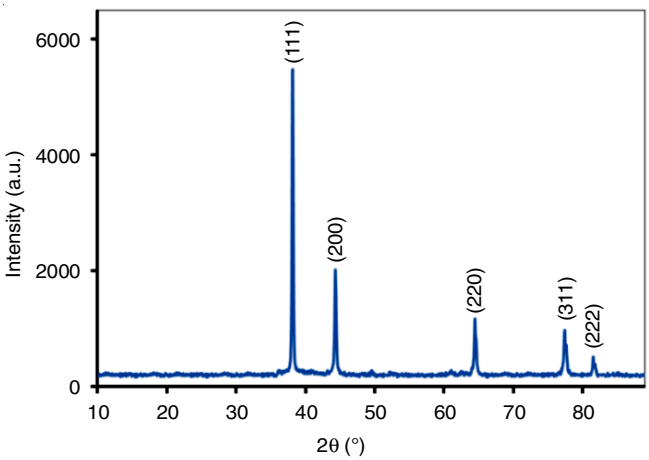

Fig. 2. XRD patterns of *CI*-AgNPs

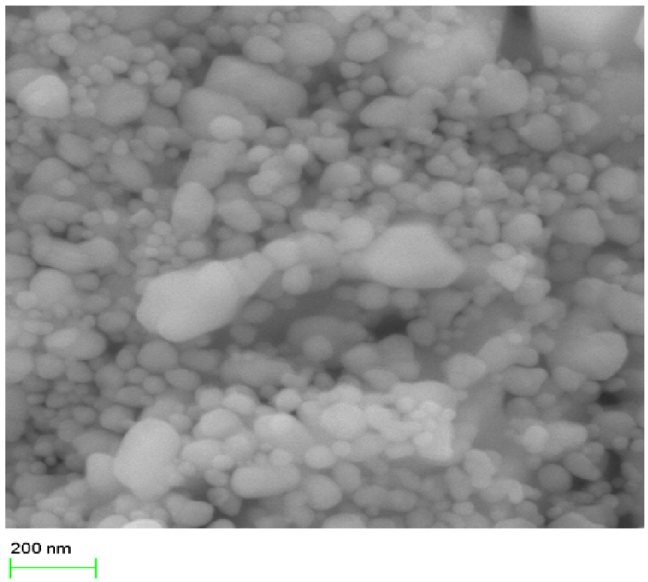

Fig. 3. SEM images of *CI*-AgNPs

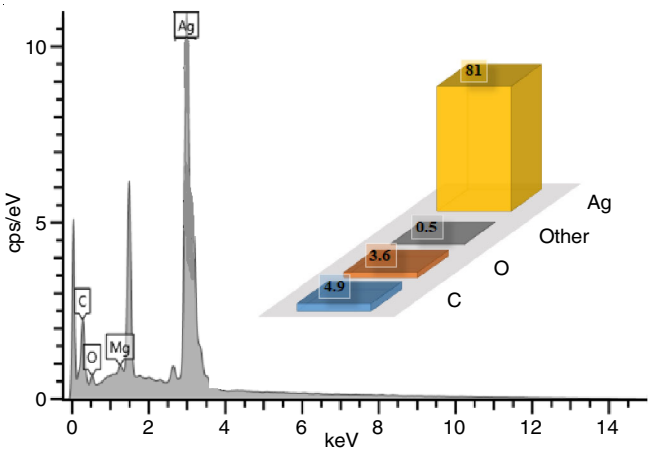

Fig. 4. EDX spectra of *CI*-AgNPs

(TEM) (Fig. 5). Moreover, the LPSA analysis exhibited an average size of 48 ± 0.06 nm (Fig. 6). The TEM images and LPSA indicated that the nanoparticle size was lower than 50 nm. The nanoparticle size and shape varied according to the applied green extract.

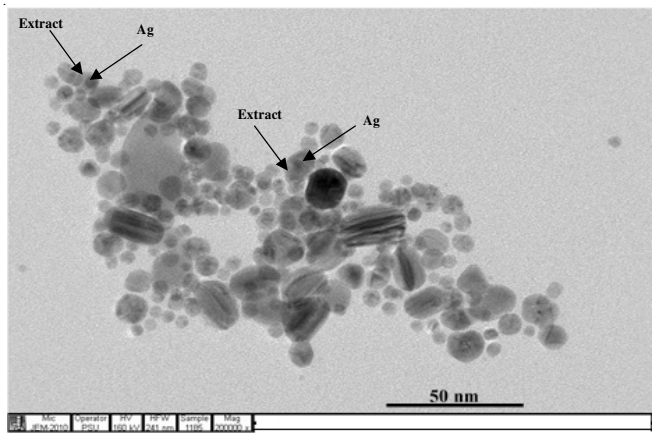

Fig. 5. TEM images of *CI*-AgNPs

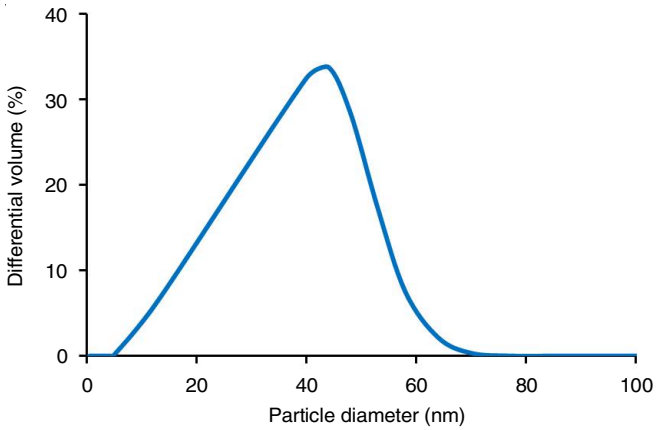

Fig. 6. LPSA spectra of *CI*-AgNPs

FTIR studies: The FTIR spectrum of *C. indicum* leaf extract (Fig. 7) presented the characteristic absorption peaks for C-N stretching (aliphatic amines), C-H group (aromatic) [37], C=O stretching [38] and O-H stretching [39]. These absorption peaks were found at 1042, 1350, 1561 and 3400 cm^{-1}, respectively. FTIR analysis confirmed the presence of phenolic compounds as the major components in the leaf extract. The FTIR spectrum of the *CI*-AgNPs exhibited a broad peak intensity decrease at around 3400 cm^{-1}; this could be due to the -OH stretch vibration in the phenolic compounds.

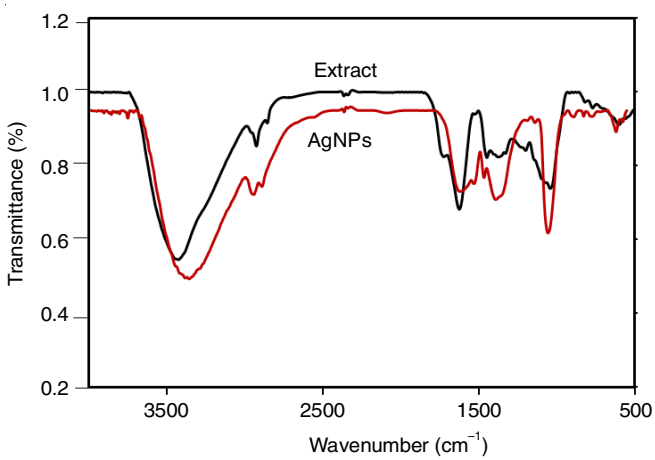

Fig. 7. FTIR spectroscopy of the leaf extract and *CI*-AgNPs

The shift to a lower wavelength could be due to the presence of an OH functional group, which induces the reduction of the Ag^+ ions [40].

Antioxidant activity: The antioxidant activity of *CI*-AgNPs was measured using the DPPH scavenging assay (Fig. 8a). The IC_{50} value of the *CI*-AgNPs was 15.13 mg/mL (Fig. 8b). The result revealed that the *CI*-AgNPs possessed an antioxidant activity similar to that of the control, ascorbic acid (IC_{50} value of 10.41 mg/mL). The functional groups of *CI*-AgNPs could be responsible for the antioxidant ability. The AgNPs synthesized using the aqueous leaf extract of *Parkia speciosa* exhibited radical scavenging activity by the DPPH assay and the IC_{50} value was 15.26 µg/mL [41]. In another study, the AgNPs synthesized from *Lactobacillus brevis* MSR104 demonstrated antioxidant activity and a great scavenging activity against the DPPH free radicals and nitric oxide free radicals [42].

Antibacterial activity: The antimicrobial activity of the *CI*-AgNPs was determined by the agar well diffusion methodology. Here, both *E. coli* (Gram-negative) and *S. aureus* (Gram-positive) were used for testing. The results indicated an efficient antimicrobial activity of the *CI*-AgNPs against *E. coli* and *S. aureus*. The maximal growth inhibition was 13.5 ± 0.50 mm and 17 ± 0.40 mm, respectively (Table-2) when compared to that of the distilled water as the control. Moreover, the mean inhibition zone for the Gram-positive bacteria was larger than that in the Gram-negative bacteria. The mechanism of antibacterial action of the AgNPs against these bacteria may involve their attachment to the cell membrane. This might lead to the subsequent destruction of permeability and respiration of the organisms. Small nanoparticles with larger surface areas provide more antibacterial activity than those provided by the larger nanoparticles [43]. Morones *et al.* [44] studied the characteristics of AgNPs using EDS and TEM and found that the AgNPs attach to the cell membrane surface and penetrate inside the bacterial cell. They may destroy the cell because the Ag^+ ions can interact with the cell proteins, similar to sulfur and phosphorus molecules present in the DNA. Moreover, AgNPs have been synthesized using the microorganism *L. brevis* MSR104 isolated for antimicrobial action. Thus, the synthesized AgNPs presented outstanding antibacterial action against Gram-negative and Gram-positive and the activity was dependent on the dose of the AgNPs [42].

TABLE-2
ANTIMICROBIAL ACTIVITY OF THE AgNPs SYNTHESIZED FROM THE *C. indicum* LEAF EXTRACT

Agent	Mean diameter of inhibition zone (mm)	
	Gram-negative (*E. coli*) bacteria	Gram-positive (*S. aureus*) bacteria
CI-AgNPs	13.50 ± 0.50	17.00 ± 0.40
Leaf extract	No inhibition	No inhibition
$AgNO_3$	9.50 ± 0.50	10.00 ± 0.50
DW	No inhibition	No inhibition

Dye degradation: The catalytic activity of *CI*-AgNPs was investigated by degrading methylene blue under simulated solar irradiation. The absorption decreased at the wavelength of 664 nm and over 90% of methylene blue was degraded after 90 min (Fig. 9). Increasing the reaction time helped in the degradation of methylene blue dye. The AgNPs synthesized using *Parkia speciosa* aqueous leaf extract also possessed the ability to degrade methylene blue under solar irradiation [41]. The degradation of the dye pollutants in a photocatalytic decomposition procedure is mostly due to the photogeneration of an electron-hole pair between the valence bands and conduction. The other probable reason for the degradation of methylene blue is that it is electroactive; hence, it can receive electrons and degrade into colourless leucomethylene blue (LMB) [45].

Conclusion

In this study, AgNPs were successfully synthesized using the *C. indicum* leaf extract, which acted as the capping agent and reducing agent. SEM, TEM images and LPSA analysis demonstrated that the average size of spherical-like AgNPs was about 25-50 nm. The antioxidant activity of the synthesized *CI*-AgNPs demonstrated an IC_{50} value of 15.13 µg/mL. These nanoparticles displayed an efficient and effective antimicrobial activity against *S. aureus* and *E. coli*. Additionally, the synthesized *CI*-AgNPs were capable of degrading methylene blue dye.

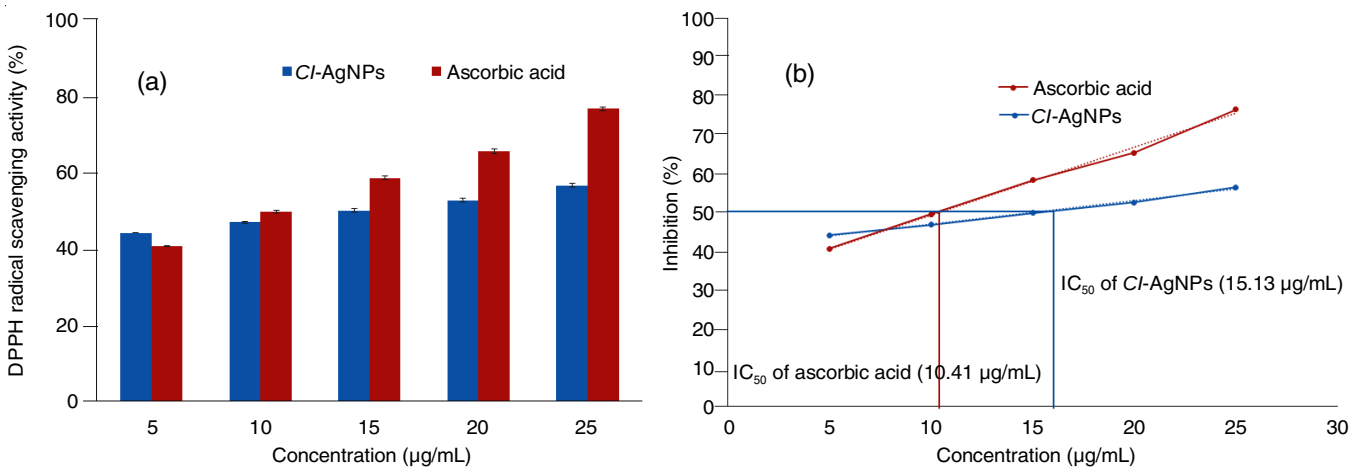

Fig. 8. DPPH radical scavenging activity of ascorbic acid and *CI*-AgNPs (a) and the IC_{50} values for the radical scavenging activities of ascorbic acid and *CI*-AgNPs (b)

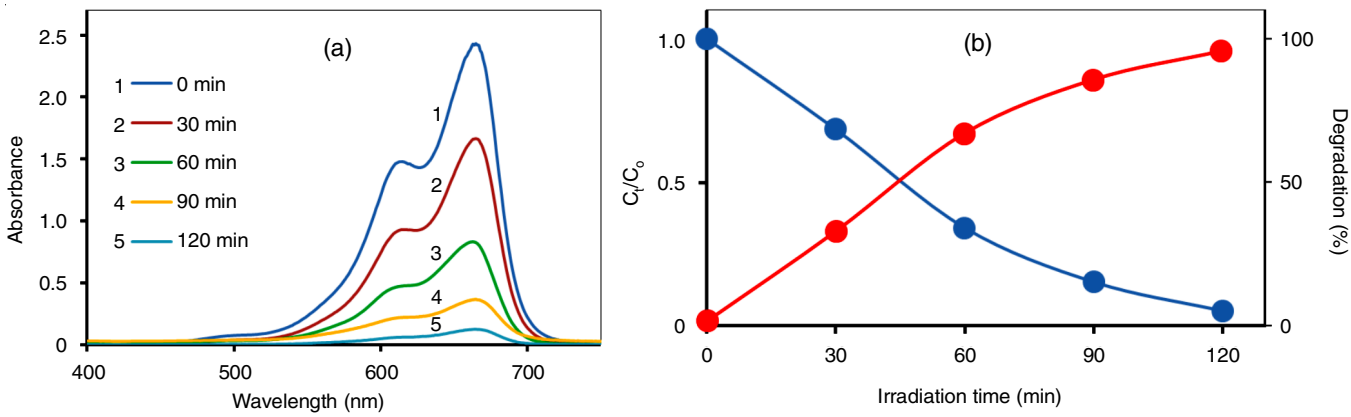

Fig. 9. (a) UV-vis spectrum for the degradation of methylene blue dye; and (b) degradation(%) against time (min)

ACKNOWLEDGEMENTS

This research was financially supported by Nanomaterials Chemistry Research Unit, Department of Chemistry, Faculty of Science and Technology, Nakhon Si Thammarat Rajabhat University, Nakhon Si Thammarat, Thailand.

CONFLICT OF INTEREST

The authors declare that there is no conflict of interests regarding the publication of this article.

REFERENCES

1. C. Gkanatsiou, Ê. Karamanoli, U. Menkissoglu-Spiroudi and C. Dendrinou-Samara, *Polyhedron*, **170**, 395 (2019); https://doi.org/10.1016/j.poly.2019.06.002
2. I. Kumar, M. Mondal, V. Meyappan and N. Sakthivel, *Mater. Res. Bull.*, **117**, 18 (2019); https://doi.org/10.1016/j.materresbull.2019.04.029
3. M. Ali, B. Kim, K. D. Belfield, D. Norman, M. Brennan and G.S. Ali, *Mater. Sci. Eng.*, **58**, 359 (2016); https://doi.org/10.1016/j.msec.2015.08.045
4. A. Heuer-Jungemann, N. Feliu, I. Bakaimi, M. Hamaly, A. Alkilany, I. Chakraborty, A. Masood, M.F. Casula, A. Kostopoulou, E. Oh, K. Susumu, M.H. Stewart, I.L. Medintz, E. Stratakis, W.J. Parak and A.G. Kanaras, *Chem. Rev.*, **119**, 4819 (2019); https://doi.org/10.1021/acs.chemrev.8b00733
5. M.K. Carpenter, T.E. Moylan, R.S. Kukreja, M.H. Atwan and M.M. Tessema, *J. Am. Chem. Soc.*, **134**, 8535 (2012); https://doi.org/10.1021/ja300756y
6. B. Demirkan, S. Bozkurt, A. Savk, K. Cellat, F. Gülbagca, M.S. Nas, M.H. Alma and F. Sen, *Sci. Rep.*, **9**, 12258 (2019); https://doi.org/10.1038/s41598-019-48802-0
7. M. Yasir, J. Singh, M.K. Tripathi, P. Singh and R. Shrivastava, *Pharmacogn. Mag.*, **13**, S840 (2018).
8. F. Göl, A. Aygün, A. Seyrankaya, T. Gür, C. Yenikaya and F. Sen, *Mater. Chem. Phys.*, **250**, 123037 (2020); https://doi.org/10.1016/j.matchemphys.2020.123037
9. M.S. Mohseni, M.A. Khalilzadeh, M. Mohseni, F.Z. Hargalani, M.I. Getso, V. Raissi and O. Raiesi, *Biocatal. Agric. Biotechnol.*, **25**, 101569 (2020); https://doi.org/10.1016/j.bcab.2020.101569
10. P. Mohanpuria, N.K. Rana and S.K. Yadav, *J. Nanopart. Res.*, **10**, 507 (2008); https://doi.org/10.1007/s11051-007-9275-x
11. N. Toropov and T. Vartanyan, Materials Science Comprehensive Nanoscience and Nanotechnology, Elsevier, Edn 2, vol. 1, 61 (2019).
12. M. Hamelian, M.M. Zangeneh, A. Shahmohammadi, K. Varmira and H. Veisi, *Appl. Organomet. Chem.*, **34**, e5278 (2020); https://doi.org/10.1002/aoc.5278
13. P. Porrawatkul, R. Pimsen, S. Chanthai and P. Nuengmatcha, *Asian J. Chem.*, **32**, 2079 (2020); https://doi.org/10.14233/ajchem.2020.22749
14. M.A. Ebrahimzadeh, S. Mortazavi-Derazkola and M.A. Zazouli, *J. Mater. Sci. Mater. Electron.*, **30**, 10994 (2019); https://doi.org/10.1007/s10854-019-01440-8
15. A. Noypha, Y. Areerob, S. Chanthai and P. Nuengmatcha, *J. Korean Ceram. Soc.*, **58**, 297 (2021); https://doi.org/10.1007/s43207-020-00096-z
16. L. Faxian, L. Jie and C. Xueling, *Rare Met. Mater. Eng.*, **46**, 2395 (2017); https://doi.org/10.1016/S1875-5372(17)30204-7
17. M.K. Rabinal, M.N. Kalasad, K. Praveenkumar, V.R. Bharadi and A.M. Bhikshavartimath, *J. Alloys Compd.*, **562**, 43 (2013); https://doi.org/10.1016/j.jallcom.2013.01.043
18. X. Zhang, H. Sun, S. Tan, J. Gao, Y. Fu and Z. Liu, *Inorg. Chem. Commun.*, **100**, 44 (2019); https://doi.org/10.1016/j.inoche.2018.12.012
19. A. Arya, V. Mishra and T.S. Chundawat, *Chem. Data Coll.*, **20**, 100190 (2019); https://doi.org/10.1016/j.cdc.2019.100190
20. R.A. Hamouda, M. Abd El-Mongy and K.F. Eid, *Microb. Pathog.*, **129**, 224 (2019); https://doi.org/10.1016/j.micpath.2019.02.016
21. M.A. Ebrahimzadeh, A. Naghizadeh, O. Amiri, M. Shirzadi-Ahodashti and S. Mortazavi-Derazkola, *Bioorg. Chem.*, **94**, 103425 (2020); https://doi.org/10.1016/j.bioorg.2019.103425
22. P. Wetwitayaklung, T. Phaechamud, C. Limmatvapirat and S. Keokitichai, *Acta Hortic.*, 185 (2008); https://doi.org/10.17660/ActaHortic.2008.786.20
23. S. Sanguri, S. Kapil, P. Gopinathan, F.K. Pandey and T. Bhatnagar, *Environ. Ecol.*, **29**, 1351 (2011).
24. Y. Yadav, P.K. Mohanty and S.B. Kasture, *Int. J. Pharm. Life Sci.*, **2**, 687 (2011).
25. V.A. Bairagi, N. Sadu, K.L. Senthilkumar and Y. Ahire, *Int. J. Pharm. Phytopharmacol. Res.*, **1**, 166 (2012).
26. B.S. Barik, S. Das and T. Hussain, *Eur. J. Med. Plants*, **31**, 87 (2020); https://doi.org/10.9734/ejmp/2020/v31i2030369
27. J. Sahu, P.K. Patel and B. Dubey, *Int. J. Pharm. Res. Dev.*, **4**, 86 (2012).
28. T. Efferth, S. Kahl, K. Paulus, M. Adams, R. Rauh, H. Boechzelt, X. Hao, B. Kaina and R. Bauer, *Mol. Cancer Ther.*, **7**, 152 (2008); https://doi.org/10.1158/1535-7163.MCT-07-0073
29. S.U. Ganaie, T. Abbasi and S.A. Abbasi, *Particulat. Sci. Technol.*, **36**, 681 (2018); https://doi.org/10.1080/02726351.2017.1292336
30. G.E. Trease and W.C. Evans, Pharmacognosy, Saunders Publishers: London; Edn. 15, pp. 42-44. 221-229, 246-249, 304-306, 331-332, 391-393 (2002).
31. J.B. Harborne, Phytochemical Methods: A Guide to Modern Techniques in Plants Analysis, Chapman & Hall: London, Edn 2, pp. 1-10, 100-117 (1984).

32. W. Brand-Williams, M.E. Cuvelier and C. Berset, *LWT-Food Sci. Technol.*, **28**, 25 (1995); https://doi.org/10.1016/S0023-6438(95)80008-5
33. T.M. Jasiem, I.S. Abbas and S.S. Raoof, *J. Glob. Pharma Technol.*, **10**, 267 (2018).
34. M.A. Odeniyi, V.C. Okumah, B.C. Adebayo-Tayo and O.A. Odeniyi, *Sustain. Chem. Pharm.*, **15**, 100197 (2020); https://doi.org/10.1016/j.scp.2019.100197
35. R. Bhat, V.G. Sharanabasava, R. Deshpande, U. Shetti, G. Sanjeev and A. Venkataraman, *J. Photochem. Photobiol. B*, **125**, 63 (2013); https://doi.org/10.1016/j.jphotobiol.2013.05.002
36. P. Mulvaney, *Langmuir*, **12**, 788 (1996); https://doi.org/10.1021/la9502711
37. S. Das, J. Das, A. Samadder, S.S. Bhattacharyya, D. Das and A.R. Khuda-Bukhsh, *Colloids Surf. B Biointerfaces*, **101**, 325 (2013); https://doi.org/10.1016/j.colsurfb.2012.07.008
38. S. Dinesh, S. Karthikeyan and P. Arumugam, *Arch. Appl. Sci. Res.*, **4**, 178 (2012).
39. T.Y. Suman, S.R. Radhika Rajasree, A. Kanchana and S.B. Elizabeth, *Colloids Surf. B Biointerfaces*, **106**, 74 (2013); https://doi.org/10.1016/j.colsurfb.2013.01.037
40. R. Vivek, R. Thangam, K. Muthuchelian, P. Gunasekaran, K. Kaveri and S. Kannan, *Process Biochem.*, **47**, 2405 (2012); https://doi.org/10.1016/j.procbio.2012.09.025
41. V. Ravichandran, S. Vasanthi, S. Shalini, S.A.A. Shah, M. Tripathy and N. Paliwal, *Results Phys.*, **15**, 102565 (2019); https://doi.org/10.1016/j.rinp.2019.102565
42. M.S. Riaz Rajoka, H.M. Mehwish, H. Zhang, M. Ashraf, H. Fang, X. Zeng, Y. Wu, M. Khurshid, L. Zhao and Z. He, *Colloids Surf. B Biointerfaces*, **186**, 110734 (2020); https://doi.org/10.1016/j.colsurfb.2019.110734
43. A. Panáèek, L. Kvítek, R. Prucek, M. Koláø, R. Veèeøová, N. Pizúrová, V.K. Sharma, T. Nevìèná and R. Zboøil, *J. Phys. Chem. B*, **110**, 16248 (2006); https://doi.org/10.1021/jp063826h
44. J.R. Morones, J.L. Elechiguerra, A. Camacho, K. Holt, J.B. Kouri, J.T. Ramírez and M.J. Yacaman, *Nanotechnology*, **16**, 2346 (2005); https://doi.org/10.1088/0957-4484/16/10/059
45. Y. Ma, F. Shi, Z. Wang, M. Wu, J. Ma and C. Gao, *Desalination*, **286**, 131 (2012); https://doi.org/10.1016/j.desal.2011.10.040